Protein Binding onto Surfactant-Based Synthetic Vesicles

ARTICLE *in* THE JOURNAL OF PHYSICAL CHEMISTRY B · MARCH 2007

Impact Factor: 3.3 · DOI: 10.1021/jp0646067 · Source: PubMed

Protein Binding onto Surfactant-Based Synthetic Vesicles

Caterina Letizia,[†] Patrizia Andreozzi,[†] Anita Scipioni,[†] Camillo La Mesa,*[,†,‡] Adalberto Bonincontro,[‡,§] and Elisabetta Spigone[§]

Department of Chemistry, SOFT-INFM-CNR Research Centre, and CNISM-Department of Physics, La Sapienza University, P. le A. Moro 5, I-00185 Rome, Italy

Received: July 20, 2006; In Final Form: November 6, 2006

Synthetic vesicles were prepared by mixing anionic and cationic surfactants, aqueous sodium dodecylsulfate with didodecyltrimethylammonium or cetyltrimethylammonium bromide. The overall surfactant content and the (anionic/cationic) mole ratios allow one to obtain negatively charged vesicles. In the phase diagram, the vesicular region is located between a solution phase, a lamellar liquid crystalline dispersion, and a precipitate area. Characterization of the vesicles was performed by electrophoretic mobility, NMR, TEM, and DLS and we determined their uni-lamellar character, size, stability, and charge density. Negatively charged vesicular dispersions, made of sodium dodecylsulfate/didodecyltrimethylammonium bromide or sodium dodecylsulfate/cetyltrimethylammonium bromide, were mixed with lysozyme, to form lipoplexes. Depending on the protein/vesicle charge ratio, binding, surface saturation, and lipoplexes flocculation, or precipitation, occurs. The free protein in excess remains in solution, after binding saturation. The systems were investigated by thermodynamic (surface tension and solution calorimetry), DLS, CD, TEM, ^{1}H NMR, transport properties, electrophoretic mobility, and dielectric relaxation. The latter two methods give information on the vesicle charge neutralization by adsorbed protein. Binding is concomitant to modifications in the double layer thickness of vesicles and in the surface charge density of the resulting lipoplexes. This is also confirmed by developing the electrophoretic mobility results in terms of a Langmuir-like adsorption isotherm. Charges in excess with respect to the amount required to neutralize the vesicle surface promote lipoplexes clustering and/or flocculation. Protein−vesicle interactions were observed by DLS, indicating changes in particle size (and in their distribution functions) upon addition of LYSO. According to CD, the bound protein retains its native conformation, at least in the SDS/CTAB vesicular system. In fact, changes in the α-helix and β-sheet conformations are moderate, if any. Calorimetric methods indicate that the maximum heat effect for LYSO binding occurs at charge neutralization. They also indicate that enthalpic are by far the dominant contributions to the system stability. Accordingly, energy effects associated with charge neutralization and double-layer contributions are much higher than counterion exchange and dehydration terms.

Introduction

Vesicle-based cell-mimetic systems are interesting biochemical models and have been widely investigated in recent years.[1−5] The reasons for so much interest are many-fold. Mimicking DNA interactions with cells requires the preparation of natural or synthetic vesicles (liposomes) interacting with that biopolymer.[6−7] Unfortunately, liposomes are intrinsically metastable.[8] These are the reasons why many efforts were devoted to get "stable" vesicles, using synthetic (usually cationic) lipids[9,10] or mixing surfactants and lipids with polymers or sterols.[11−14] Such a strategy has gained renewed interest since Kaler[15] and Khan[16−18] demonstrated the possibility to form vesicles by mixing oppositely charged surfactants in non-stoichiometric ratios. Surfactant-based vesicles are thermodynamically stable,[19] and their interactions with polymers, proteins, and DNA can be investigated in equilibrium conditions.

Vesicles formed by mixing anionic and cationic surfactants, termed cat-anionic, show moderate cytotoxicity.[20] They are charged and interact with biomolecules in a wide range of pH and ionic strength values. For these reasons, cat-anionic vesicles find use as transfection vectors and replace more conventional (and costly) lipids.[21−26]

In mixed surfactant systems, the packing constraint[27] modulates the alkyl chain(s) conformation and the polar head group(s) area of the individual species and allows one to obtain supramolecular structures with proper surface charge and curvatures, including vesicles. The electrostatic contributions to the overall system stability are significant and may be properly tuned. Charges facing outside the vesicles favor their stabilization and ensure significant interactions with oppositely charged biopolymers and the formation of lipoplexes, which are promising subjects for fundamental studies, transfection technologies, and gene therapy.

Selected experimental methods give information on biopolymer binding onto vesicles and on modifications of their electrical double layer. In this regard, electrophoretic mobility and dielectric relaxation, DR, are extremely promising. The former method gives information on the mobility of the resulting supercolloids, whereas DR estimates the relaxation processes of macromolecules, proteins and DNA[28] and those pertinent to ion motion in the double layers of micelles, vesicles, and lipoplexes.[29,30]

* Corresponding author. Tel: +39-06-49913707, (direct) +39-06-491694. Fax: +39-06-490631. E-mail: camillo.lamesa@uniroma1.it.
[†] Department of Chemistry.
[‡] SOFT-INFM-CNR Research Centre.
[§] CNISM-Department of Physics.

10.1021/jp0646067 CCC: $37.00
Published on Web 01/04/2007

To get self-consistent pictures of the interactions between cat-anionic vesicles and a globular protein, lysozyme, LYSO, a systematic investigation was performed. Dynamic light scattering (DLS), ^{1}H NMR, CD, TEM, solution calorimetry, and surface tension give relevant information and support the results obtained by electrophoretic mobility and DR. The physical−chemical properties of the bare vesicles, mostly the SDS-CTAB and the SDS-DDAB ones, were also considered. Thereafter, interactions with proteins were investigated and some properties of the lipoplexes reported.

The purpose of this contribution is to shed light on unknown aspects of these systems and to define the hierarchy of forces controlling LYSO binding onto vesicles. Protein binding, insertion, and adsorption onto cells and vesicles are important tasks in biological systems. Extensive studies were performed to investigate protein adsorption onto biological surfaces (and polymeric or inorganic ones, as well), but little is known on the specific events involved in protein−surface adsorption at a molecular level and on the conformational changes that may occur. CD is a powerful method for these purposes and may determine the protein conformation in such systems.

Modeling protein adsorption in terms of simplified approaches helps to clarify its binding onto surfaces.[31−33] Binding was rationalized in terms of a Langmuir-like adsorption isotherm. It was expressed in terms of vesicle surface coverage (which is proportional to the lipoplexes charge density), and the Gibbs energy of binding was obtained. Calorimetric data support the estimates obtained by the Langmuir adsorption approximation and demonstrate that the dominant contributions to the lipoplexes stability are enthalpic.

Experimental Section

Materials. Chicken egg-white lysozyme, LYSO, Sigma, was exhaustively dialyzed in 0.15 *m* NaCl, recovered, dried, lyophilised, and kept over P_2O_5. Its ionic conductivity, density, and viscosity in bi-distilled water are in good agreement with previous data.[34,35]

Cetyltrimethylammonium bromide, CTAB, sodium dodecylsulfate, SDS, and didodecyldimethylammonium bromide, DDAB, Aldrich, were used. The absence of minima in surface tension, γ (dyne cm^{-1}), vs log *m* plots close to the respective critical micellar concentrations, CMC, confirmed their purity.[36]

Preparation of Vesicle and Lipoplexes. Solutions of the anionic and of the cationic surfactants were prepared individually and mixed together. The vesicles do form rapidly; their dispersions are fluid, slightly turbid and colored. In dilute concentration regimes DDAB gives lamellar dispersions. To overcome such difficulties, DDAB was dissolved in SDS aqueous solutions and equilibrated until the overall solution turbidity remained constant. The whole process is several hours long. The dispersions are stable, and no precipitates settle out after staying some months at room temperature. Mild centrifugation was performed, but no precipitates occur. Particularly stable are the (SDS/CTAB) [(1.7/1.0), 6.0 mmol L^{-1}], and the (SDS/DDAB) [2.5/1.0, 11.0 mmol L^{-1}] vesicular systems. The terms in parentheses indicate the mole ratio between the components. Only unilamellar vesicles, LUV, characterized by a bilayer structure, inferred by TEM, were considered. Information on the mole ratios between the components, the absolute concentrations, charge, stability, vesicle sizes, and polydispersity is summarized in Table 1.

Protein−vesicle systems were prepared by dissolving LYSO in the vesicular dispersions, under stirring. The resulting dispersions were diluted with the corresponding vesicular pseudosolvent. At (protein/vesicle) ratios less than (1.0/1.0), in terms of nominal charges, no precipitation occurs. The pH of the above mixtures was controlled by a 2000 Crison potentiometer, and is 6.5 ± 0.2, irrespective of protein content. In such pH conditions, LYSO has 8 positive charges in excess.[37] Buffers were not used, to minimize the binding of interfering ions onto LYSO, or vesicles, and to modulate their surface charge density and double layer thickness.

TABLE 1: Vesicular Systems Used, the Overall Surfactant Content (mmol kg^{-1}), the Mole Ratio between the Two Surfactants, the Surface Net Charge of the Vesicles (Inferred by ζ-Potential), the Particle Size, and the Apparent System Turbidity

mixture	surfactant content (mmol kg^{-1})	mole ratio	surface charge	particle size (nm)	turbidity
SDS/CTAB	6.0	[1.70/1.0]	-	370[a] 200−500[b]	low
SDS/CTAB	30.0	[1.70/1.0]	-		high
SDS/DDAB	11.0	[2.50/1.0]	-	240[a] 150−300[b]	low
SDS/DDAB	25.0	[2.50/1.0]	-	260[a] 150−350[b]	low
CTAB/SOS	20.0	[1.33/1.0]	+	300−1200[b]	low to high[c]

[a] Average particle size obtained by DLS. [b] The particle size distribution width was inferred by TEM. [c] Vesicles precipitate out to within some days.

Methods. *Dielectric Relaxation.* The permittivity, ϵ', and loss, ϵ'', were measured by 4194A and 4192A H.P. impedance analyzers in the range of 10^5-10^9 Hz. The errors on ϵ' and ϵ'' are ±2.0 and ±4.0%, respectively. The measuring cell is the section of a cylindrical waveguide,[38] operating beyond its cutoff frequency. The cell constants were determined by standard procedures.[39] The relaxing contribution to the dielectric loss is $\epsilon_d'' = \epsilon'' - \chi/\epsilon_o\omega$, where χ is the ionic conductivity, $\omega = 2\pi f$, the angular frequency of the applied electric field, and ϵ_o is the dielectric constant of vacuum. The experiments were performed at 25.0 ± 0.1 °C.

Electrophoretic Mobility. A Malvern laser-velocimetry Doppler utility, of the HT ZS Nano series, determined the electrophoretic mobility, μ, by taking the average of several individual scans. The solutions were located in U-shaped cuvettes, equipped with gold electrodes. The temperature was set to 25.0 ± 0.1 °C. Before performing the measurements, the apparatus performances were checked by determining the electrophoretic mobility of LYSO at different pH values.[40] μ values were taken at the maximum of the intensity-distribution function (in number of counts) vs the applied voltage, *V*. The distribution functions are narrow. Data were transformed into ζ-potential ones according to[41]

$$\zeta = \left[\frac{4\pi\eta\mu}{\epsilon E}\right] \quad (1)$$

where ζ is the ζ-potential, ϵ is the dielectric constant of the medium, *E* is the applied electric field, and η is the solvent viscosity. Errors on μ values are ±3%. Equation 1 is valid in the Smoluchowskij approximation (i.e., when the screening length is much lower that the particle radius).[41] Such requirements are fulfilled in the present experimental conditions, since vesicles and lipoplexes are hundreds of nanometers in diameter. Estimates calculated by assuming the residual charge on the vesicles to be equal to the surfactant concentration in excess give Debye screening lengths, $1/\kappa$, in the 3−5 nm range. Surface conductance terms were not considered, since the corrections proposed by Lyklema[42] did not improve the mobility results.

When sedimentation is significant, noticeable drifts complicate the instrumental response, and the measured values are not reliable.

Dilution Enthalpy. The batch solution calorimeter, working at 25.00 ± 0.01 °C, is of the heat conduction type, LKB mod. 2107. A cooling circulator, LKB 2210, a control unit, LKB 2107-350, and a potentiometric recorder, LKB 2110, were used. More details are reported elsewhere.[43] The apparatus performances were calibrated with aqueous sucrose.[44] Dilution enthalpies, Q_{meas}, were obtained by multiplying the calibration constant, θ, and the integral area on the recorder, A. Integral enthalpies of dilution, $\Delta H_{i,dil}$ (J mol^{-1}) were obtained by

$$\Delta H_{int,dil} = \left[\frac{Q_{meas}}{n}\right] \quad (2)$$

where n is the mole number of solute. The uncertainty on $\Delta H_{i,dil}$ values is ±1.0%.

Surface Activity. Measurements were performed by a Kruss K10T unit, equipped with a Du Noüy ring, which was flamed, cleaned with 1.0 *m* HCl, and washed with doubly distilled water. The temperature in the vessel is 25.0 ± 0.1 °C. The surface tensions of doubly distilled water and of absolute ethanol (γ = 72.0 dyne cm^{-1}, and 21.8 dyne cm^{-1} at 25.0 °C, respectively)[45] were used in the calibration. In the preparation of vesicles, SDS micellar solutions were added with progressive amounts of aqueous CTAB. To minimize drifts due to adsorption kinetics, the measurements were performed 10 min after addition of each aliquot. γ values are the average of five independent runs, and the accuracy is ±0.2 dyne cm^{-1}.

Circular Dichroism. A JASCO spectropolarimeter, mod. J 810, equipped with 450 W xenon lamps, performed the measurements. The bandwidth resolution is between 0.01 and 0.15 nm, and the minimum ellipticity is 5×10^{-3} millideg cm^{-1}. The temperature is 25.0 ± 0.1 °C. Measurements were performed in cells of 0.01, or 0.2 cm, path length, to minimize the scattering due to the solution turbidity. The experiments were run in the 190−280 nm range, where LYSO has peculiar absorption bands at 208 and 222 nm.[46]

Laser Light Scattering. A Brookhaven digital correlator (BI 9000AT), equipped with a 632.8 nm 10 mW He−Ne laser source, performed DLS experiments at 90°. The samples were located in cuvettes, at 25.00 ± 0.05 °C. The detection unit consists of a photomultiplier and an amplifier, working as pulse selectors. Details on the apparatus and on the measuring procedures are given elsewhere.[47] The relaxation times, (1/Γ), were determined by a *CONTIN* program, working in terms of a continuous distribution of exponential decay-times.[48] Errors in the average particle size were ±5%.

The Malvern Zetasizer unit, Nano ZS series HT, performed additional DLS measurements in back mode, at 173° and 25.0 ± 0.1 °C, at the same wavelength. A CONTIN data analysis facility, available in the apparatus programs, elaborated the decay-time distribution functions. The agreement between the two sets of data is within ±5%.

NMR. A Bruker AVANCE AQS600 spectrometer operating at 600 MHz on ^{1}H performed NMR experiments, at 300.0 K. It is equipped with a multinuclear *z*-inverse probe head, Bruker, producing gradients of 55 G cm^{-1}. Standard pulse sequences were used.[49] The number of scans was adjusted to achieve good signal-to-noise ratios. When required, a soft presaturation of HOD signals was applied. Details on the data elaboration and more information on operative conditions are reported elsewhere.[50]

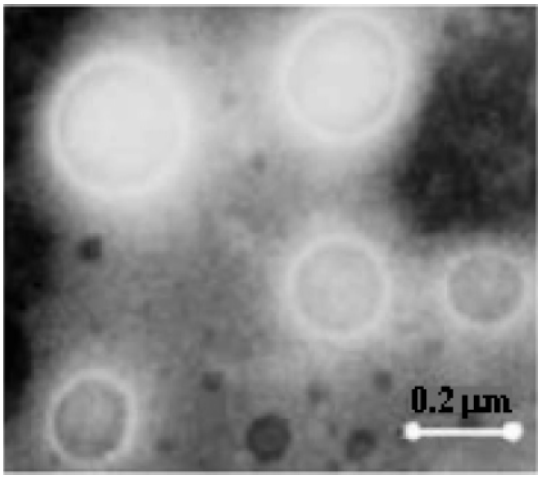

Figure 1. TEM image of vesicular (SDS/CTAB) dispersions. The overall surfactant content is 6.0 mmol kg^{-1} and the ratio between the two (1.70/1.00). Bars in the bottom of the figure give estimates of the vesicles size.

TEM. Drops of the vesicular dispersions were adsorbed onto carbon-coated copper grids and allowed to adhere. Dispersion in excess was removed by filter paper. A drop of 1.0 wt % phosphotungstic acid solution was added and the liquid in excess removed. The samples were dried and observed by a ZEISS EM 900 electron microscope, at 80 kV.[51] Examples indicating the occurrence of large uni-lamellar vesicles are reported in Figure 1.

Ionic Conductivity. A 6425 precision component analyzer, Wayne-Kerr, was used. The measuring cell is located in an oil bath, at 25.000 ± 0.003 °C. Measurements were performed by adding known amounts of (CTAB) solutions to micellar SDS by a weight burette, under stirring, and recorded 10 min after each addition. Significant changes in slope indicate vesicles formation.

Solution Viscosity. Capillary viscometers were located in a water bath at 25.00 ± 0.01 °C. Density measurements were made by an A. Paar DMA 60 unit at 25.00 ± 0.01 °C. Relative viscosities, η_{rel}, are inferred by the ratio ($t\rho/t°\rho°$), where t and $t°$ are the flow times and ρ and $\rho°$ are the densities of the mixtures and of the mother SDS micellar solution, respectively. They are accurate to ±0.5%. The onset of vesicles is concomitant to changes in slope of η_{rel} values.

Results

Partial Phase Diagram. The phase boundaries and the region of existence of vesicular dispersions for cat-anionic systems are known.[17,52,53] Information available on the water−sodium dodecylsulfate-cetyltrimethylammonium bromide one refers only to the formation of mixed micelles.[54] This system was investigated in more detail, and the region where vesicles occur was defined. The partial phase diagram in Figure 2 indicates that the vesicular region is located between a precipitate area, a lamellar liquid crystalline dispersion, and a solution region. The location of the vesicular region in the phase diagram is similar to structurally related systems.[55,56]

Some macroscopic properties of the surfactant solutions change on going from the micellar to the vesicular region. For instance, vesicle dispersions are turbid and slightly colored, compared to micellar solutions. To define in more detail the region where vesicles occur DLS, turbidity, and surface tension were used. The micelle−vesicle transitions are not true phase boundaries and, according to DLS, both kinds of aggregates

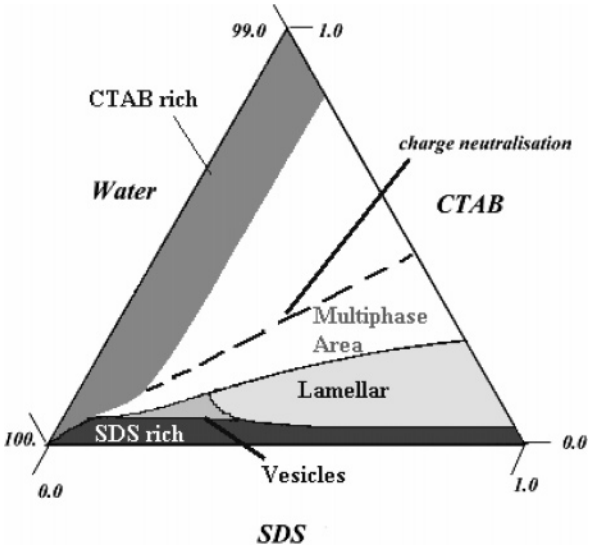

Figure 2. Partial phase diagram of the system water−SDS−CTAB, at 25.0 °C. The vesicle region is in middle gray. It is surrounded by a multiphase area, in white, by a micellar region, dark gray, and by a lamellar dispersion, light gray. The solution region in the CTAB-rich part of the phase diagram is indicated in medium dark gray.

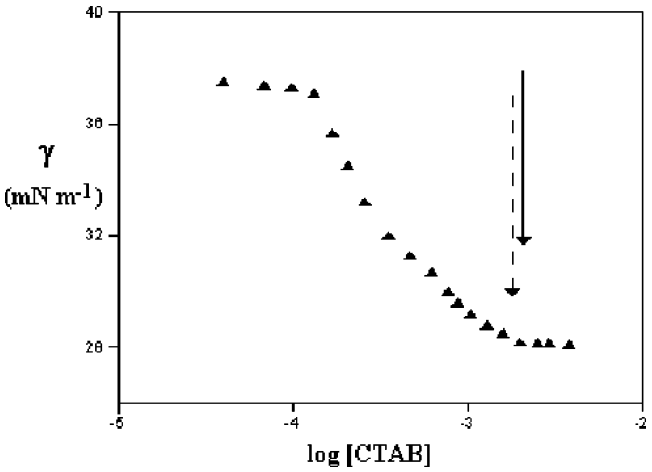

Figure 3. Dependence of surface tension, γ (dyne cm^{-1}) of a 10.0 mmol kg^{-1} SDS micellar solution on added CTAB, at 25.0 °C. The plateau on the right indicates vesicles formation. The arrows indicate the micelle−vesicle transitions inferred by conductivity, dotted line, and viscosity, full line.

coexist in solution. The micelle−vesicle transition, promoted by adding aqueous CTAB to micellar SDS, is concomitant to a significant decrease in surface tension and is followed by a plateau, Figure 3. This behavior finds correspondence with the low surface tension values observed in lamellar liquid crystalline dispersions (N.B. Vesicles are lamellar structures).[57] Vesicular dispersions have γ values in the range of 26.0−29.0 dyne cm^{-1}, whereas in the corresponding micellar solutions, they are close to ≈35−37 dyne cm^{-1}. Ionic conductivity and solution viscosity, too, do significantly change on adding CTAB, Figure 3.

Vesicle Size and Charge Density. The vesicle sizes were inferred by DLS and TEM. According to TEM, uni-lamellar vesicles, LUV, dominate over multilamellar ones. The *z*-average diameter, D_z, and the size-distribution width of LUV's are reported in Table 1. A perusal to that table indicates that the sizes range from 150 to about 1300 nm, and depend significantly on the (anionic/cationic) mole ratio. In Figure 4 is reported the nice correspondence between charge ratio and the width of the distribution function for the different vesicular systems. Such

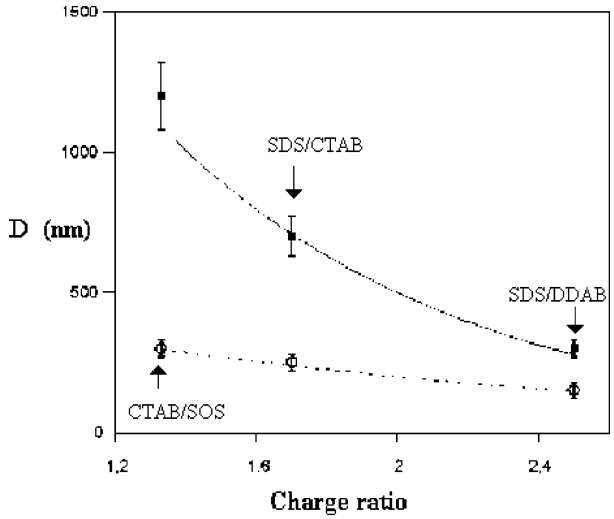

Figure 4. Dependence of the lower, ○, and upper, ■, vesicle size, *D* (nm), on the charge ratio for the systems (CTAB/SOS), (SDS/CTAB), and (SDS/DDAB), respectively. The width of the distribution functions is proportional to the distance between two such lines. The particles sizes were inferred by TEM.

an effect has never received due attention. Vesicle stability changes from system to system; the most stable dispersions are the (SDS/DDAB) and the (SDS/CTAB) ones.

The electrophoretic mobility of vesicular dispersions, μ, depends on the overall surfactant content and on the (anionic/cationic) mole ratio. Surfactant in excess determines the vesicle charge and the resulting mobility is $\gtrless 0$. High charge ratios imply high mobility (in modulus). The width of the corresponding distribution function decreases on increasing the charge ratio.

Protein−Vesicle Interactions. Addition of LYSO to vesicular dispersions is concomitant with significant changes in structural, transport and thermodynamic properties. Some aspects of the protein-vesicle systems are reported below.

Particle Size. In Figure 5, panels A and B, the sizes and their distribution functions for vesicles and lipoplexes are reported. DLS indicates that added LYSO promotes the formation of lipoplexes in both vesicular systems. There are some differences on the growth mechanism, indeed. When the overall LYSO content is below the charge neutralization, a significant increase in size compared with the bare vesicles and a shrinking of the corresponding distribution functions are observed in the (SDS/CTAB) and in the (SDS/DDAB) systems. Slightly above that limit, the lipoplexes flocculate and the solution turbidity increases. Lipoplexes precipitation is slow, if any, since surface charges in excess stabilize them. Above neutralization the particle size increases, and the width of its distribution functions widens. The LYSO−(SDS/DDAB) system, conversely, shows two populations without added protein, a drift in turbidity close to the neutralization point, and the occurrence of relatively fast sedimentation processes above it (5 min). Monodisperse lipoplexes are obtained after sedimentation has occurred, see the bottom image in Figure 5A.

LYSO binds to vesicles, reduces their surface charge density, σ, and modifies the medium ionic strength, *I*. Binding controls the charge density and the double layer thickness. The weight of these contributions is hardly quantified, and we assume, in a first approximation, the former effect to be dominant.

NMR data support the occurrence of large particles, with presence of wide bands in the spectra, resulting from the overlapping of many classes of protons, Figure 6. The large

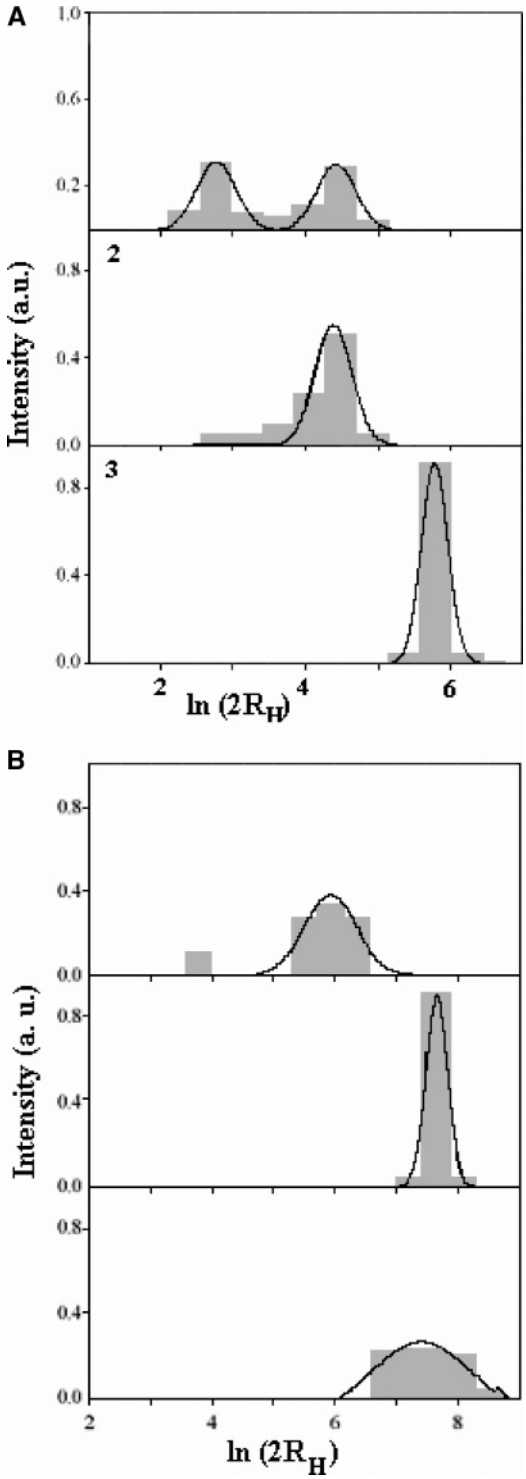

Figure 5. (A) Plot of the intensity distribution function, I (a.u.), obtained by DLS for vesicular dispersion as a function of particle diameter (in nm), at 25.0 °C. From the top data refer to 25.0 mmol kg^{-1} (SDS/DDAB) and (2.5/1.0) mole ratios, and to the same mixture with 0.12 (below the saturation threshold) and 0.45 mmol kg^{-1} LYSO (above the saturation threshold). (B) Plot of the intensity distribution function, I (in a.u.), for (SDS/CTAB) vesicles, 6.0 mmol kg^{-1} and (1.7/1.0) mole ratio. From the top, without protein, with 1.4 (below the saturation threshold) and 1.4 mmol kg^{-1} added LYSO (above the saturation threshold), respectively.

and poorly resolved ^{1}H spectral profiles indicate that the surfactants experience restricted motion. The observed super-Lorentian band shapes are quite similar to those relative to long rod-like micelles.[58,59] The signals ascribed to the protein are poorly resolved, too, Figure 6C. NMR, thus, gives merely qualitative indications on the occurrence of large particles.

Support to the above hypothesis comes from electrophoretic mobility measurements. The interactions between vesicles and proteins find analogy with the titration of charged particles by oppositely charged species.[60] Addition of LYSO implies significant changes in μ values, which progressively reduce and approach zero. When saturation is complete, μ values change in sign and remain constant. This behavior is ascribed to the presence of free LYSO. Data in Figure 7 indicate that ζ vs [LYSO] plots are not symmetric with respect to the isoelectric point. Such evidence supports surface saturation, the formation of lipoplexes, and occurrence of positively charged species (lysozyme, very presumably) above neutralization. The surface charge density of protein-coated vesicles, σ, was obtained by rewriting the ζ-potential equation as

$$\sigma = \left[\frac{\epsilon\zeta}{4\pi\tau}\right] = \left[\frac{\eta\mu}{\tau E}\right] \tag{3}$$

where τ is the effective double layer thickness around the lipoplexes. To avoid unrealistic estimates for τ, which depend on the medium ionic strength, eq 3 is rewritten as[41]

$$\sigma\tau = \left[\frac{\epsilon\zeta}{4\pi}\right] = \left[\frac{\eta\mu}{E}\right] \tag{4}$$

and is expressed as electric moment per unit area. Such value can be derived with respect to the amount of added protein; it depends on changes in surface charge density and in the double layer thickness as well. When ζ approaches zero, the same holds for the product ($\sigma\tau$). In that limit, the surface charge density approaches zero and the double layer thickness, obviously, diverges. For a demonstration, see the Appendix.

As to interfacial polarization and the associated dielectric relaxation processes, reported in Figure 8, the data were fitted into a Cole−Cole equation,[61] according to

$$\epsilon - \epsilon_\infty = \left[\frac{\Delta\epsilon}{1 + \left(\frac{jf}{f^*}\right)^{(1-\alpha)}}\right] \tag{5}$$

where ϵ is the complex dielectric permittivity of the mixtures, f and f^* are the measuring and relaxation frequencies, respectively, j is the imaginary unit, $\Delta\epsilon$ is the dielectric increment, ϵ_∞ is the high-frequency permittivity, and α is an empirical parameter related to the spreading of relaxation times. More details on the elaboration procedures are given elsewhere.[30]

The dynamic processes associated with the orientational relaxation of LYSO in solution fulfill eq 5 but are observed in a quite different frequency range, compared to the vesicular systems. Their amplitude, $\Delta\epsilon$, is a linear function of protein content, and the relaxation frequency in water is constant and close to 9 MHz.[62] It is possible, therefore, to detect the occurrence of free protein, once vesicle saturation has occurred. Saturation occurs at the salient point of $\Delta\epsilon$ vs added protein plot, Figure 9. The same holds for the relaxation frequency plot, in the same figure.

Let us discuss, in the following, the behavior observed in the LYSO−(SDS/CTAB) system. No significant dielectric increment of the vesicular dispersions compared to water occurs in the available frequency range. The classical Maxwell−Wagner double-layer relaxation processes occur at much lower frequencies, because of the vesicle size.[63] In presence of small amounts of LYSO, the interfacial polarization processes are traceless up to the charge neutralization. When LYSO content

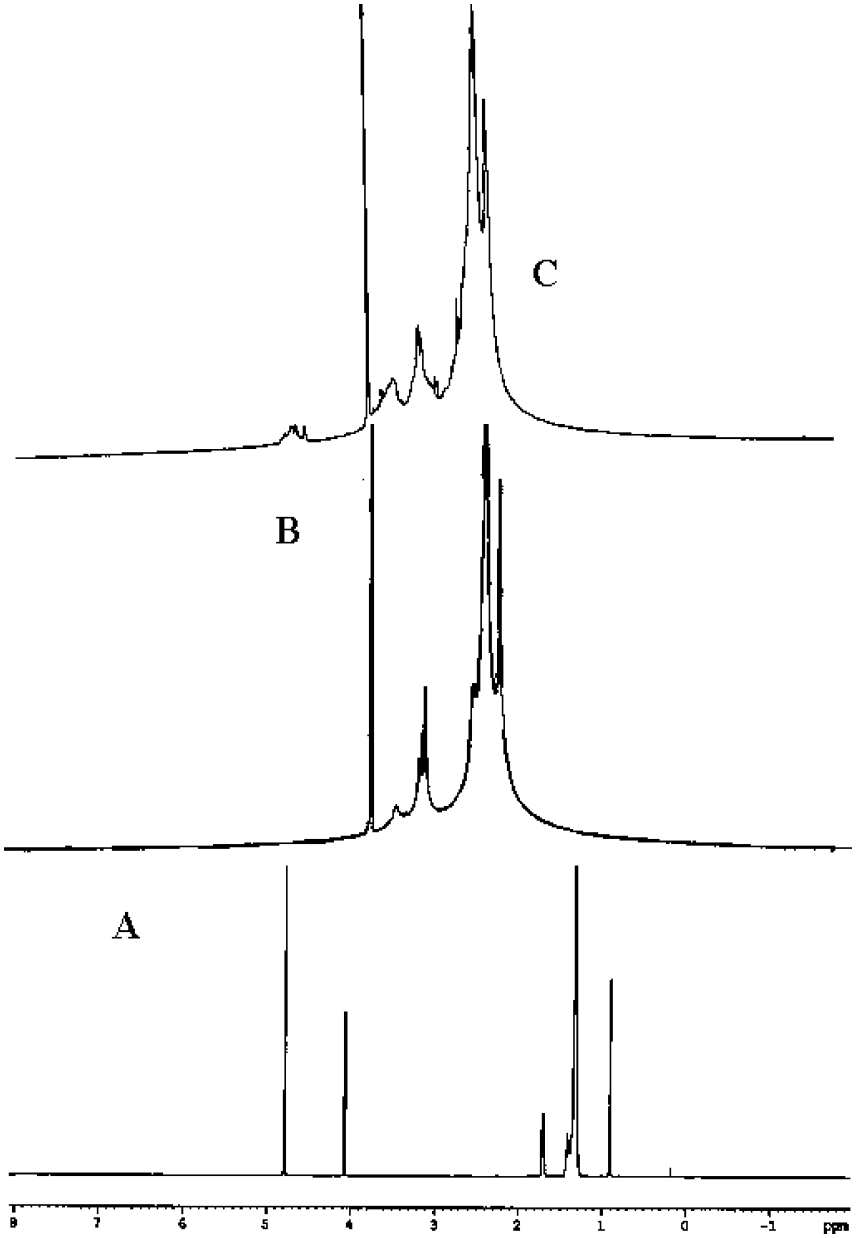

Figure 6. ^{1}H NMR spectra of a 20.0 mmol kg^{-1} SDS solution, A, a 25.0 mmol kg^{-1} (SDS/DDAB) vesicular dispersion, (2.5/1.0) mole ratio, B, and of the same dispersion after addition of 0.21 mmol kg^{-1} LYSO, C. The experiments were performed in D_2O, at 300 K.

is in excess with respect to that value, relaxing contributions of the free protein occur, Table 2 and Figure 9. From the above data, it comes out that the dielectric relaxation amplitude scales with the amount of LYSO in excess, whereas the vesicle-bound one is traceless.

Conversely, the (SDS/DDAB) system shows interfacial polarization contributions at ≈500 kHz. They progressively reduce upon addition of the protein, reach a minimum, and increase again when LYSO concentration is higher than the neutralization threshold, Table 2. In this system, the relaxing amplitudes and frequencies are not directly related to the amount of free protein. A complete surface charge neutralization does not occur, and $\Delta\epsilon$ never reaches zero. Addition of LYSO results in a nonlinear combination of different relaxation processes. Tentative explanations for the differences observed in the two systems could be as follows. In the (SDS/CTAB) system, the protein is located into an extended double layer, having nearly the same permittivity as water. In the (SDS/DDAB) one, conversely, LYSO lies in a double layer, whose permittivity is largely different from that of bulk H_2O.

The ζ-potential and DR give proofs on the interaction processes, when calorimetry quantifies their strength. Very small changes in pH (to within ±0.2 units) were observed upon mixing with vesicles, and the calorimetric values do not contain significant contributions due to LYSO deprotonation. The apparent molal enthalpy of dilution for the protein, (where $\Delta H_{int,dil} = \Phi_{L,fin} - \Phi_{L,in}$) and the partial molal values, were analyzed according to

$$\Phi_L = \sum_{i=1} A_i m^{i/2} \tag{6}$$

$$L_2 = \left(\frac{\partial(\Phi_L m^{1/2})}{\partial m^{1/2}}\right) \tag{7}$$

where Φ_L and L_2 are the apparent and partial molal enthalpies

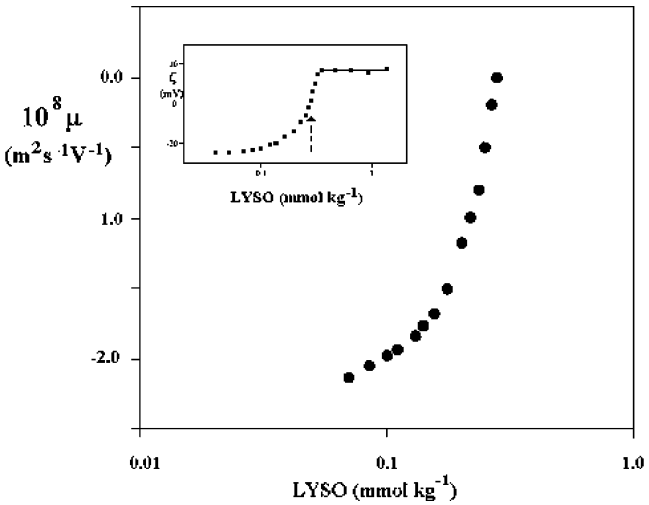

Figure 7. Electrophoretic mobility, μ, 10^8 m^2 s^{-1} V^{-1}, vs added LYSO, (mmol kg^{-1}), in semilogarithmic scale. Data refer to concentrations below the charge neutralization limit. In the inset are reported the ζ-potential values, in mV, vs added LYSO, at 25.0 °C. Saturation is concomitant to a change in slope and is indicated by an arrow. The dispersion is the (SDS/CTAB) one, 6.0 mmol kg^{-1} and (1.7/1.0) mole ratio.

of dilution for LYSO in the vesicular solvent, respectively, m is the protein molality, and other terms are constants. The A_1 term in eq 6 was calculated according to Debye−Hückel theory, to account for the medium polarizability.[64] Other constants were obtained from a polynomial fitting procedure, as exhaustively indicated in previous work.[43] The integral enthalpies of dilution of LYSO in pure water were also measured, Figure 10.

A steep discontinuity in L_2 values was observed by adding LYSO to the vesicular pseudosolvent. At the neutralization threshold, the interaction enthalpy, ΔH_{int}, is −47.0 kJ mol^{-1}, Figure 10. Such a value implies the presence of large enthalpic contributions and indicates that the release from vesicles is energetically un-favored. Above saturation, water, free LYSO, lipoplexes, and electrolytes coexist. In fact, the slope of the function above the vesicle neutralization threshold is close to that pertinent to free lysozyme. The difference between L_2 values in such a regime corresponds to the transfer enthalpy of LYSO to lipoplexes containing solvent. The results indicate that terms relative to charge neutralization and double layer interactions are relevant. Attempts to quantify the weight of enthalpic and entropic terms are made below.

Proteins interacting with molecular surfactants denature, loosing their secondary and tertiary structures.[65,66] No such evidence has been reported in protein−vesicle systems, and CD measurements were performed. The spectra reported in Figure 11 indicate that LYSO retains its α-helix conformation. The positions of the minima at 208 and 222 nm are less intense compared to native LYSO; perhaps, the amount of α-helix and β-sheet conformations (inferred by a CONTIN algorithm) is quite close to it. Changes in intensity of the absorbing bands may be due to solution turbidity or partial sedimentation of the lipoplexes. There are some differences in the two vesicular pseudo-solvents. The (SDS/CTAB)-based system does not give significant protein denaturation, whereas changes in α-helix and β-sheet conformation in the (SDS/DDAB)-based one are larger. The effects responsible for that behavior may be due to the ionic strength of the vesicular media or to differences in the interaction strength.

The results relative to the (SDS/CTAB)-based system are self-consistent. The behavior observed in the (SDS/DDAB) system,

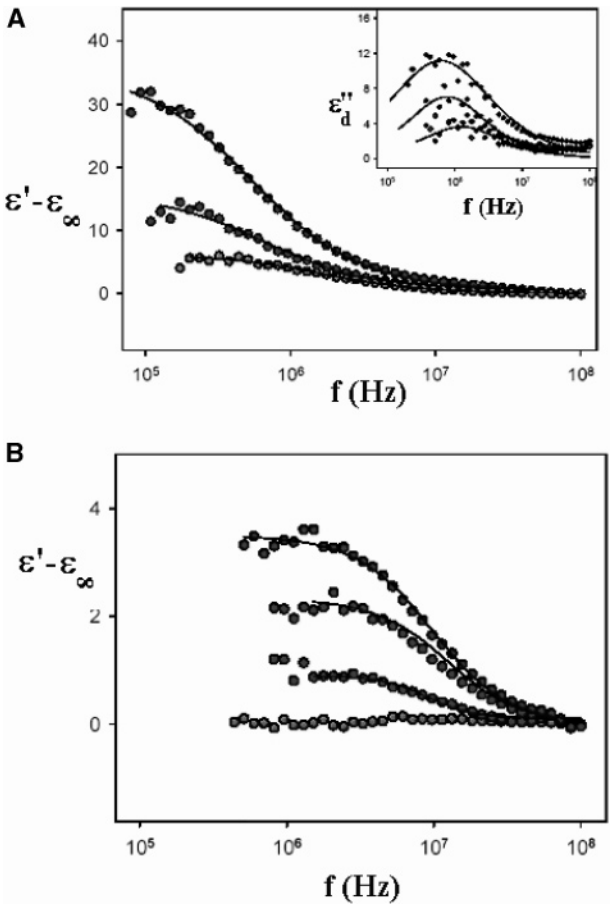

Figure 8. (A) Dielectric relaxation spectra of the (SDS/DDAB) system, 11.0 mmol kg^{-1} and (2.5/1.0) mole ratio, at 25.0 °C. The data, reported as $\epsilon' - \epsilon_\infty$ vs log f (MHz), refer to bare vesicles, with 0.15 and 0.28 mmol kg^{-1} added LYSO, from the top. In the inset is reported the imaginary dielectric component of the mixtures, ϵ''_d. (B) Relaxation spectra in the (SDS/CTAB) system, 6.0 mmol kg^{-1} and (1.7/1.0) mole ratio, at 25.0 °C. From the bottom, data indicate the bare vesicles, with 0.42, 0.82, and 1.40 mmol kg^{-1} added LYSO, respectively. Note the different amplitudes compared to panel A. The errors on ϵ''_d are large, since ionic contributions are dominant, and the imaginary spectra are not reported.

conversely, shall not be discussed, since CD indicates the occurrence of some conformational changes. In addition, lysozyme binding onto vesicles implies significant precipitation and does not allow one to determine the interaction enthalpy. Furthermore, the difficulties in determining the electrophoretic mobility of the lipoplexes and the dielectric relaxation processes do not permit us to develop the simplified Langmuir model for protein adsorption.

Discussion

Protein binding onto cat-anionic vesicles is concomitant with modifications in many physical−chemical properties. The analysis of experimental data gives information on crucial aspects of a complex behavior. Information can be obtained on (i) protein binding onto vesicles, or insertion into bilayers, (ii) protein−vesicle interaction energy, (iii) conformation of vesicle-bound protein, (iv) modifications in the surface charge density, and (v) formation and fusion of lipoplexes.

The properties of the original vesicles were properly tuned, so that the dominant interaction modes with the protein involved, essentially, electrostatics. As a reminder, the absence of buffers is justified by the need to maximize double layer effects. The electrostatic interactions between macromolecules and vesicles,

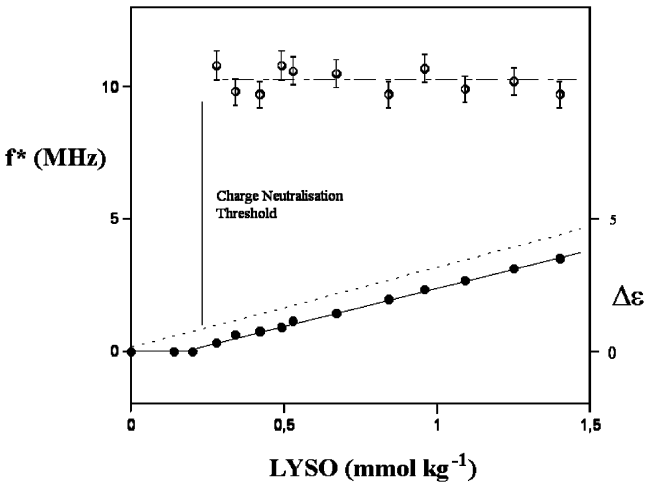

Figure 9. Dependence of the relaxation amplitude, $\Delta\epsilon$, ●, right scale, and frequency, f^*, (MHz), ○, on added lysozime, (mmol kg^{-1}), for the (SDS/CTAB) system, 6.0 mmol kg^{-1} and (1.7/1.0) mole ratio, at 25.0 °C. The errors on f^* are indicated as bars, and those on $\Delta\epsilon$ are lower than the symbol size. The dotted line indicates the dielectric increment of LYSO in net water and the vertical one the saturation threshold.

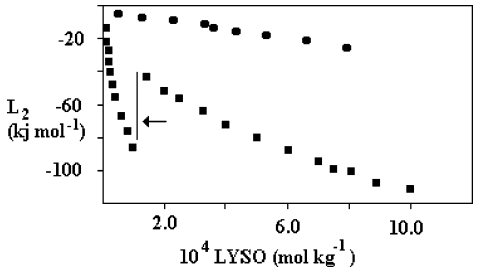

Figure 10. Plot of the partial molal enthalpy of dilution, L_2 (in kJ mol^{-1}) vs lysozyme molality, at 25.00 °C, ■. The steep change, indicated by a vertical bar, corresponds to the saturation point. The interaction enthalpy, ΔH_{int}, is the difference between the two branches of the curve. It is indicated by an arrow. L_2 for LYSO in water is indicated by full circles.

in fact, can be analyzed in terms of a Langmuir-like adsorption isotherm or by more refined Goüy−Chapman approaches.[67−69] Conversely, the use of Freundlich and Dubinin−Radushkevich isotherms is suitable when binding is controlled by the ionic strength.[70]

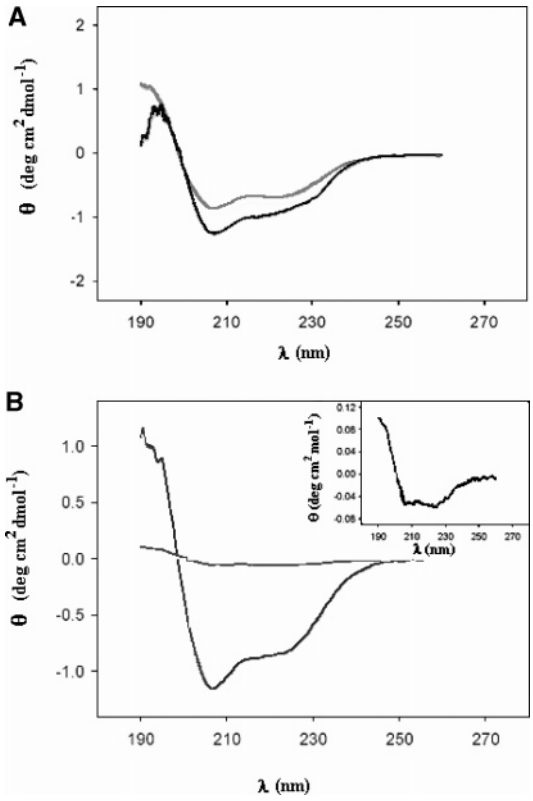

Figure 11. (A) CD spectra, reported as θ, in 10^{-6} deg cm^2 dmol^{-1}, vs λ, in nm, for the (SDS/CTAB) system, 6.0 mmol kg^{-1} and (1.7/1.0) mole ratio, with 0.14, black, and 0.80, gray, mmol kg^{-1} LYSO, at 25 °C. (B) CD spectra in the (SDS/DDAB) system, 25.0 mmol kg^{-1} and (2.5/1.0) mole ratio, at 25 °C. The solutions contain 0.09, black, and 0.18, gray, mmol kg^{-1} LYSO. The latter spectrum is magnified in the inset. Note the differences with panel A.

Protein Binding and/or Insertion. Binding consists in a uniform coverage of charged surfaces by small poly ions. According to studies on cytochrome *c* adsorption onto liposome's, binding conforms to a Langmuir adsorption isotherm.[71,72] It is not site-specific (i.e., all binding sites on the vesicles are equivalent) and depends on the surface size, charge, and protein content, as well. The process continues until all uniformly smeared-out charges on the vesicles are neutralized.

TABLE 2: Concentration of Added Lysozyme, [LYSO], in mmol kg^{-1}, the Dielectric Increment, $\Delta\epsilon$, the Relaxation Frequency, f^*, (MHz), and the Dispersion Term, α, Relative to the (SDS/CTAB) System, 6.0 mmol kg^{-1}, (1.7/1.0) Mole Ratio, Left, and to the (SDS/DDAB) One, 11.0 mmol kg^{-1}, (2.5/1.0) Mole Ratio, Right, at 25.0 °C, Calculated by Best Fitting Procedures Based on eq 5[a]

[(SDS/CTAB), 6.0 mmol kg^{-1}, (1.7/1.0)]				[(SDS/DDAB), 11.0 mmol kg^{-1}, (2.5/1.0)]			
[LYSO] (mM)	$\Delta\epsilon$	f^* (MHz)	α	[LYSO] (mM)	$\Delta\epsilon$	f^* (MHz)	α
0.00				0.00	36.0 ± 1	0.54 ± 0.03	0.23 ± 0.02
0.14				0.15	16.0 ± 0.9	0.69 ± 0.07	0.23 ± 0.04
0.20				0.28	6.3 ± 0.3	1.6 ± 0.1	0.20 ± 0.03
0.28	0.32 ± 0.03	10.8 ± 0.7	0.22 ± 0.07	0.33	4.1 ± 0.4	1.6 ± 0.3	0.23 ± 0.07
0.34	0.62 ± 0.03	9.8 ± 0.5	0.11 ± 0.04	0.43	3.7 ± 0.2	1.8 ± 0.2	0.20 ± 0.04
0.42	0.75 ± 0.05	9.8 ± 0.6	0.14 ± 0.06	0.49	3.0 ± 0.2	1.7 ± 0.2	0.20 ± 0.07
0.49	0.92 ± 0.08	10.8 ± 0.8	0.10 ± 0.08	0.55	5.4 ± 0.3	1.1 ± 0.1	0.24 ± 0.02
0.53	1.16 ± 0.07	10.6 ± 0.7	0.23 ± 0.05	0.61	9.0 ± 0.6	0.83 ± 0.09	0.19 ± 0.02
0.67	1.45 ± 0.08	10.5 ± 0.7	0.24 ± 0.05	0.70	13.1 ± 0.6	0.66 ± 0.05	0.23 ± 0.03
0.84	1.96 ± 0.08	9.7 ± 0.4	0.23 ± 0.04	0.76	14.1 ± 0.8	0.62 ± 0.07	0.25 ± 0.03
0.96	2.35 ± 0.10	10.7 ± 0.5	0.22 ± 0.03	0.81	16.5 ± 0.7	1.3 ± 0.1	0.22 ± 0.04
1.09	2.67 ± 0.09	9.9 ± 0.3	0.25 ± 0.03	0.94	15.3 ± 0.6	1.3 ± 0.1	0.27 ± 0.03
1.25	3.09 ± 0.12	10.2 ± 0.5	0.21 ± 0.04	1.10	15.7 ± 0.5	1.23 ± 0.07	0.30 ± 0.02
1.40	3.52 ± 0.10	9.7 ± 0.4	0.22 ± 0.03	1.24	16.2 ± 0.6	1.30 ± 0.09	0.30 ± 0.03
				1.39	15.0 ± 1	1.3 ± 0.2	0.33 ± 0.04

[a] Errors are indicated.

Insertion into bilayers, conversely, is concomitant to a rearrangement of the vesicles, with formation of holes having the same size as the protein. The energy of the latter process is ascribed to the work required entering the vesicles and is counteracted by potential barriers. Conformational changes in the protein are a prerequisite for its insertion in the bilayers.[73]

In a first approximation, we do not account for the mobility of surfactant ions onto vesicles,[74] transmembrane potentials,[75] conformation of the adsorbed protein,[76] flip-flop,[77] apoptosis,[78] and pynocytosis,[79] which allow the translocation across the bilayers. In fact, the relaxation times of flip-flop mechanisms have high activation energy and are much longer than the rates of local motion.[80] They are traceless in the measurements reported here. In addition, apoptosis and pynocytosis require significant modifications in the vesicle curvature and, according to TEM, are not effective. Variations in transmembrane potentials could not be observed by the present experiments.

Globular proteins prefer adsorption to insertion, up to a threshold where the chemical potential of the adsorbed species overcomes the work required for their insertion into bilayers. Conformational changes favor insertion, since the protein outer surface becomes more hydrophobic compared to the native conformation.[81,82] Very few efforts have been devoted on these lines, as in cytochrome *c* binding to lipid bilayers.[83,84] This protein enters the bi-layers, depending on the intrinsic binding constant, K_0, on the medium ionic strength, I, and on surface coverage, θ_s.

Let us consider a binding model based on electrophoretic mobility results, where protein−vesicle interactions are analyzed in terms of a Langmuir-like approximation. LYSO is considered a spherical uniformly charged particle of 3−4 nm in diameter,[85] and its binding is rationalized in terms of hard-spheres absorption onto large surfaces. The charge density of vesicles with proteins adsorbed is expressed as[83,84]

$$\sigma = \left(1 - \frac{Z\theta_s}{N}\right)\left(\frac{e}{f_0}\right) \tag{8}$$

where Ze is the effective charge on LYSO, at the given pH, N isthe number of molecules of area f_0 having one charge, and θ_s is the fractional coverage of the vesicle surface. (e/f_0) is the surface charge density per binding site, σ_0. Proper rearrangement of eq 8 gives

$$1 - \left(\frac{\sigma}{\sigma_0}\right) = \sigma_{red} = \left(\frac{Z}{N}\right)\theta_s \tag{9}$$

which accounts for the links between charge density and surface coverage. In this model, the counter-ions condensation onto vesicles is not explicitly accounted for.

The binding constant to a given site, K_0, can be expressed as

$$K_0 \cong [X^+]\left(1 - \frac{Z\theta_s}{N}\right)^{-2Z} = [X^+](1 - \sigma_{red})^{-2Z} \tag{10}$$

where $[X^+]$ is the concentration of released counter-ions. The charge density of the lipoplexes is obtained by a smeared-out value, calculated by a mean-field approximation,[86] and the adsorption isotherm can be written as

$$K_0(\mathrm{LYSO}) = \{[X^+](1 - \sigma_{red})^{-2Z}\} \left\{\left(\frac{\theta_s}{1-\theta_s}\right)\exp\left(\frac{\theta_s}{1-\theta_s}\right)\exp\left(\frac{3-2\theta_s}{1-\theta_s}\right)\right\} \tag{11}$$

where the second term in brackets accounts for adsorption. The binding constant calculated by eq 11 is reported in Figure 12 as a function of θ_s. The above equation gives the Gibbs energy of binding, $\Delta G_{bind} = RT \ln K_0(\mathrm{LYSO})$, which is about −50 kJ mol^{-1}, close to the ΔH_{int} value inferred by calorimetry. Differences between the two quantities are moderate (2−3 kJ mol^{-1}) and indicate that entropic contributions to binding are ancillary, if any. Binding proceeds up to surface saturation and levels off above it. Multilayer binding, with consequent flocculation of the lipo-plexes, occurs when LYSO in excess remains in solution.

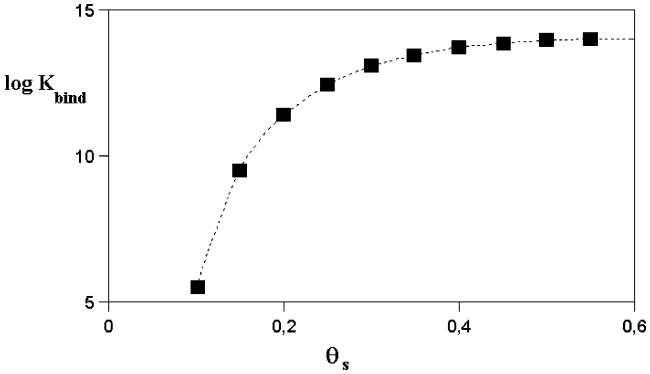

Figure 12. Plot of the equilibrium constant, K_0, calculated by eqs 10 and 11, vs the vesicle surface coverage by adsorbed LYSO, θ_s. Data refer to the (SDS/CTAB) system, 6.0 mmol kg^{-1} and (1.7/1.0) mole ratio.

Binding implies significant changes in many other properties. In particular, the $\Delta\epsilon$ (LYSO) function is parallel to that of the molecular solution, Figure 9. The protein in excess remains in solution and no further adsorption occurs. No changes in LYSO conformation were inferred from the dielectric relaxation frequency.[62] Thus, the LYSO−(SDS/CTAB) system can be modeled according to a surface saturation of large vesicles by oppositely charged proteins.[87] The model has significant analogies with that experimentally observed in the binding of ferritin to large, surface-modified vesicles.[88]

Interaction Energy. Studies on protein adsorption demonstrate the importance of enthalpic contributions (vdW, electrical double layer, and hydrophobic ones). Entropically based mechanisms, conversely, control the release of counter-ions, of solvation water, and modify ordered structures, due to adsorption-induced conformational changes.[89] In the limits set up by the present procedures, no pH and conformational changes in the protein occur, and the observed effects are ascribed to binding. The enthalpic effect is some kJ mol^{-1}, since each protein occupies adjacent sites. Hydrophobic contributions to the interaction may occur[90] but are not consistent with CD findings. Entropic terms are moderate, despite ion and water exchange from the vesicles.

Bound Protein Conformation. The amount of α-helix conformation was determined in water and in vesicles. In water the fractions of α-helix and β-sheet conformation are 0.34 and 0.17, respectively; the remaining part is due to the turn + random coil terms.[46] In the (SDS/CTAB) vesicular dispersions, the α-helix contribution decreases to 0.32, leaving unchanged the weight of the β-sheet one. In the (SDS/DDAB) system, the conformational changes are 0.28 and 0.21, for α-helix and β-sheet conformations, respectively. There are, presumably, some links between protein conformation and binding strength. The small variations observed in the (SDS/CTAB) system do not support the occurrence of conformational changes. It can be safely assumed that the protein retains its native conformation

and that no bi-layer insertion occurs. Such an eventuality would be concomitant with conformational changes and has not been observed.

The behavior reported here is different from that observed in surfactant solutions. At concentrations below the CMC, proteins denature and the amount of α-helix conformation drops.[91] Micelle-assisted redissolution implies a recovery of the native conformation (but not the tertiary structure), and the protein is in a molten-globule state.[92] The differences between cat-anionic systems and micelles are rationalized if the molecular surfactant is responsible for protein denaturation.[93] In cat-anionic mixtures, the amount of molecular surfactant is orders of magnitude lower than in micellar solutions,[94,95] and very tiny amounts of both surfactants exist in disperse form.

Modifications in the Vesicles State of Charge. Protein binding finds analogy with the titration of particles by oppositely charged polyelectrolytes.[96] The process continues up to neutralization and subsequent flocculation or precipitation. In LYSO-containing systems, the charges not directly involved in binding stabilize the lipoplexes. This behavior is similar to that reported in DNA compaction onto vesicles.[7] At this stage, it is hazardous to ascertain whether the stabilization due to vesicle-bound biopolymers is ubiquitous.

Formation and Fusion of Lipoplexes. According to the ζ-potential, binding is nearly stoichiometric. The protein favors the formation of lipoplexes. The process is concomitant with a significant increase in particle size and with a broadening in the corresponding distribution function. In our opinion, charges in excess on the lipoplexes surface are responsible for their nucleation, and for the significant resistance to sedimentation.

Conclusions

The purpose of this contribution was to shed light on some aspects of biomimetic systems composed by vesicles and globular proteins. The justification of so much interest arises from the use of these systems in transfection technologies. Vesicular systems, differing in concentration, net charge, and size, were investigated and characterized. The main factor controlling vesicle size is the charge ratio, when the overall surfactant content is much less relevant. High charge ratios imply low polydispersity and make the vesicles stable. In a recent paper, Kaler exhaustively described the reasons for their significant thermodynamic stability.[97]

The results indicate that protein−vesicle interactions are concomitant to modifications in electrophoretic mobility and in the double layer thickness. Conformational changes subsequent to protein binding are moderate, if any. Thus, binding dominates over insertion, at least in the present experimental conditions. The interactions of vesicles with LYSO are significant and lead to the flocculation of lipoplexes. These are large objects, compared to vesicles, and have a much lower charge density.

Modeling the interactive behavior in terms of a Langmuir adsorption isotherm allows determining the surface saturation and the Gibbs energy of lysozyme binding onto vesicles, ΔG_{bind}. Calculations based on that approximation show that ΔG_{bind} is close to the interaction enthalpy, ΔH_{int}. The results presented here apply when all binding sites are equivalent, and charges in excess are homogeneously distributed onto the vesicle surface. The Langmuir approximation is justified from the size of proteins compared to vesicles.

In terms of bio-mimetic relevance, the present findings open the way to a wide number of more refined models and offer the opportunity for further investigation. From an applied viewpoint, finally, interesting indications can be given. The (SDS/CTAB) vesicular system is the most effective in terms of overall performances. The (SDS/DDAB)-based one, the most widely used up to now, does not have optimal performances, in terms of lipoplexes stability. Other vesicular systems are metastable and less reliable, because their surface charge density is too low or the overall surfactant concentration too high.

Acknowledgment. This work was supported by La Sapienza University, through a Faculty financial support. Thanks to Prof. A. L. Segre and D. Capitani, Inst. Chemical Methodologies, CNR, for help, technical assistance in performing ^{1}H NMR spectra, and fruitful discussions on some aspects of the manuscript. Thanks to Dr. R. Muzzalupo, Department Pharm. Sci., Calabria University, for help in TEM experiments. Thanks, also, to Prof. M. L. Antonelli, Department of Chemistry, La Sapienza, for allowing us the use of the calorimeter.

Appendix I

It can be demonstrated that when the ζ-potential approaches zero the same holds for its derivative with respect to the amount of added protein. Combination with eq 4 gives

$$\lim_{\zeta\to 0}\left(\frac{\eta}{\epsilon}\right)\left(\frac{\partial\zeta}{\partial C_{LYSO}}\right)=\left(\frac{\partial(\sigma\tau)}{\partial C_{LYSO}}\right)=0 \qquad (A,1)$$

where C_{LYSO} is the amount of added lysozyme. Derivation of the right-hand side term in (A,1) gives

$$\sigma\left(\frac{\partial\tau}{\partial C_{LYSO}}\right)+\tau\left(\frac{\partial\sigma}{\partial C_{LYSO}}\right)=0 \qquad (A,2)$$

Separation of variables and integration in ∂C_{LYSO} gives, after some straightforward algebra, the relation

$$\partial \ln\sigma=-\partial\ln\tau \qquad (A,3)$$

which indicates that the double layer thickness (the Debye screening length) diverges as the surface charge density, located on the shear plane of the lipoplexes, approaches zero.

References and Notes

(1) Tanford, C. *The Hydrophobic Effect and the Formation of Micelles, Vesicles and Biological Membranes*, 2nd ed.; Wiley: New York, 1980.
(2) Fendler, J. H. *Am. Chem. Soc. Symp. Ser.* **1987**, *342*, 83.
(3) Ninham, B. W.; Evans, D. F. *Faraday Disc. Chem. Soc.* **1986**, *81*, 1.
(4) Fendler, J. H. *Chem. Rev.* **1987**, *87*, 877.
(5) Evans, D. F. *The Colloidal Domain: Where Physics, Chemistry, Biology and Technology Meet*, 2nd ed.; Verlag: Heidelberg, 1998.
(6) Mel'nikov, S. M.; Dias, R.; Mel'nikova, Y. S.; Marques, E. F.; Miguel, M. G.; Lindman, B. *FEBS Lett.* **1999**, *453*, 113.
(7) Lindman, B.; Mel'nikov, S.; Mel'nikova, Y.; Nylaner, T.; Eskilsson, K.; Miguel, M.; Dias, R.; Leal, C. *Prog. Colloid Polym. Sci.* **2002**, *120*, *52*.
(8) Ferguson, C. G.; James, R. D.; Bigman, C. S.; Shepard, D. A.; Abdiche, Y.; Katsambe, P. K.; Myszka, D. G.; Prestwich, G. D. *Biocon-jugate Chem.* **2005**, *16*, 1475. Heyes, J.; Hall, K.; Taylor, Y.; Lenz, P.; Maclachlan, I. *J. Controlled Release* **2006**, *112*, 280.
(9) Eliyahu, H.; Servel, N.; Domb, A.; Barenholz, Y. *Gene Ther*. **2002**, *9*, 850.
(10) Szebeni, J.; Baranyi, L.; Savay, S.; Milosevits, J.; Bunger, R.; Laverman, P.; Metselaar, J.; Storm, G.; Chanan-Khan, A.; Liebes, L.; Muggia, F. M.; Cohen, R.; Barenholz, Y. *J. Liposome Res.* **2002**, *12*, 165.
(11) Svenson, S. *Curr. Opin. Colloid Interface Sci.* **2004**, *9*, 201.
(12) *12*) Zhai, L.; Zhao, M.; Chen, Y.; Kong, X.; Sui, W. *J. Dispers. Sci. Technol.* **2005**, *26*, 291.
(13) *13*) De Cuyper, M.; Caluwier, D.; Baert, J.; Cocquyt, J.; Van der Meeren, P. *Zh. Phys Chem.* (*Muenchen)* **2006**, *220*, 133.
(14) Muzzalupo, R.; Trombino, S.; Iemma, F.; Puoci, F.; La Mesa, C.; Picci, N. *Colloids Surf. B, Biointerfaces* **2005**, *46*, 78.

(15) Brasher, L. L.; Herrington, K. L.; Kaler, E. W. *Langmuir* **1995**, *11*, 4267.
(16) Marques, E. F.; Regev, O.; Khan, A.; Miguel, M. da G.; Lindman, B. *J. Phys. Chem. B* **1999**, *103*, 8353.
(17) Marques, E. F.; Khan, A. *Progr. Colloid Polym. Sci.* **2002**, *120*, 83.
(18) Khan, A.; Marques, E. F. *Curr. Opin. Colloid Interface Sci.* **2000**, *4*, 402.
(19) Marques, E. F. *Langmuir* **2000**, *16*, 4798.
(20) Jung-Hua, S. K.; Ming-Shiou, J.; Chien-Hsiang, C.; Hsuan-Wen, C.; Cih-Ta, L. *Colloids Surf. B, Biointerfaces* **2005**, *41*, 189.
(21) Matsui, K.; Sando, S.; Sera, T.; Aoyama, Y.; Sasaki, Y.; Komatsu, T.; Terashima, T.; Kikuchi, J.-I. *J. Am. Chem. Soc.* **2006**, *128*, 3114.
(22) Grinberg, S.; Liner, C.; Kolot, V.; Waner, T.; Wiesman, Z.; Shaubi, E.; Heldman, E. *Langmuir* **2005**, *21*, 7638.
(23) Zuidam, N. J.; Hirsch-Lerner, D.; Margulies, S.; Barenholz, Y. *Biochim. Biophys. Acta, Biomembr.* **1999**, *1419*, 207.
(24) Brohede, U.; Bramer, T.; Edsman, K.; Stromme, M. *J. Phys. Chem. B* **2005**, *109*, 15250.
(25) Song, A.; Dong, S.; Jia, X.; Hao, J.; Liu, W.; Liu, T. *Angew. Chem., Int. Ed.* **2005**, *44*, 4018.
(26) Hao, J.; Hoffmann, H. *Curr. Opin. Colloid Interface Sci.* **2004**, *9*, 279.
(27) Israelachvili, J. N.; Mitchell, D. J.; Ninham, B. W. *J. Chem. Soc. Faraday Trans. 1* **1976**, *72*, 1525.
(28) Bonincontro, A.; Cametti, C.; Nardiello, B.; Marchetti, S.; Onori, G. *Biophys. Chem.* **2006**, *121*, 7.
(29) Barchini, R.; Pottel, R. *J. Phys. Chem.* **1994**, *98*, 7899.
(30) Bonincontro, A.; Michiotti, P.; La Mesa, C. *J. Phys. Chem. B* **2003**, *107*, 14164.
(31) Latour, R. A., Jr.; Trembley, S. D.; Tian, Y.; Lickfield, G. C.; Wheeler, A. P. *J. Biomed. Mater. Res.* **2000**, *49*, 58.
(32) Bayramoglu, G.; Arica, M. Y. *Colloids Surf., A: Physicochem. Eng. Aspects* **2002**, *202*, 41.
(33) Lopez Valdivieso, A.; Reyes Bahena, J. L.; Song, S.; Herrera Urbina, R. *J. Colloid Interface Sci.* **2006**, **298**, 1.
(34) Zielenciewicz, A. *J. Therm. Anal. Calor.* **2001**, *65*, 467.
(35) Monkos, K. *Biochim. Biophys. Acta: Prot. Struct. Mol. Enzymol.* **1997**, *1339*, 304.
(36) Mysels, K. J.; Florence, A. T. *J. Colloid Interface Sci.* **1973**, *48*, 410.
(37) Moernstam, B.; Wahlund, K. G.; Jönsson, B. *Anal. Chem.* **1997**, *69*, 5037.
(38) Bonincontro, A.; Briganti, G.; Giansanti, A.; Pedone, F.; Risuleo, G. *Colloids Surf. B, Bionterfaces* **1996**, *6*, 219.
(39) Athey, T. W.; Stuckly, M. A.; Stuckly, S. S. *IEEE Trans. Microwave Theory Tech.* **1982,** *30*, 82.
(40) Sarmiento, F.; Ruso, J. M.; Prieto, G.; Mosquera, V. *Langmuir* **1998**, *14*, 5725.
(41) Adamson, A. W. *Physical Chemistry of Surfaces*, 5th ed.; Wiley & Sons: New York, 1990; Chapter V, p 203.
(42) van der Wal, A.; Minor, M.; Norde, W.; Zehnder, A. J. B.; Lyklema, J. *Langmuir* **1997,** *13*, 165.
(43) Capalbi, A.; Gente, G.; La Mesa, C. *Colloids Surf. A: Physicochem. Eng. Asp.* **2004,** *246*, 99.
(44) Wadso, I. *Acta Chem. Scand.* **1968**, *22*, 927. Monk, P.; Wadso, I. *Acta Chem. Scand.* **1968**, *22*, 1942.
(45) *Handbook of Chemistry an Physics*, 61th ed.; CRC Press: Boca Raton, FL, 1980; Tab. F45. Azizian, S.; Hemmati, M. *J. Chem. Eng. Data* **2003**, *48*, 662.
(46) Ikeda, K.; Hamaguchi, K. *J. Biochem. (Tokyo)* **1970**, *68*, 785.
(47) Bordi, F.; Cametti, C.; Di Biasio, A.; Angeletti, M.; Sparapani, L. *Bioelectrochemistry* **2000**, *52*, 213.
(48) Provencher, S. W. *Comput. Phys. Comm.* **1982**, *27*, 213.
(49) Braun, S.; Kalinowski, H. O.; Berger, S. *150 and more basic NMR experiments: a practical course*; Wiley−VCH: Weinheim, Germany, 1998.
(50) Sanna, C.; La Mesa, C.; Mannina, L.; Stano, P.; Viel, S.; Segre, A. L. *Langmuir* **2006**, *22*, 6031.
(51) Iemma, F., Spizzirri, U. G.; Muzzalupo, R.; Puoci, F.; Trombino, S.; Picci, N. *Colloid Polym. Sci.* **2004**, *283*, 250.
(52) Iampietro, D. J.; Kaler, E. W. *Langmuir* **1999**, *15*, 8590. See, also, ref 15.
(53) Jokela, P.; Jönsson, B.; Wennerström, H. *Progr. Colloid Polym. Sci.* **1985**, *70*, 17. Jönsson, B., Jokela, P.; Khan, A.; Lindman, B.; Sadaghiani, A. *Langmuir* **1991**, *7*, 889.
(54) Chakraborty, H.; Sarkar, M. *Langmuir* **2004**, *20*, 3551−3558.
(55) Yatcilla, M. T.; Herrington, K. L.; Brasher, L. L.; Kaler, E. W.; Chirovolu, S.; Zasadzinski, J. A. *J. Phys. Chem.* **1996**, *100*, 5874.
(56) Yu, W-Y.; Yang, Y-M.; Chang, C-H. *Langmuir* **2005**, *21*, 6185.
(57) Alexopoulos, A. H.; Franses, E. I. *Colloids Surf.* **1990**, *43*, 263. Alexopoulos, A. H.; Puig, J. E.; Franses, E. I. *J. Colloid Interface Sci.* **1989**, *128*, 26.
(58) Wennerström, H.; Ulmius, J. *J. Magn. Res.* **1976**, *23*, 431.
(59) Ulmius, J.; Wennerström, H. *J. Magn. Res.* **1977**, *28*, 309.
(60) Lopez Valdivieso, A.; Reyes Bahena, J. L.; Song, S.; Herrera Urbina, R. *J. Colloid Interface Sci.* **2006**, *298*, 1.
(61) Hasted, J. B. *Aqueous Dielectrics*; Chapman & Hall: London, 1973; Chapter I, p 24.
(62) Bonincontro, A.; Cinelli, S.; Onori, G.; Stravato, A. *Biophys. J.* **2004**, *86*, 1118.
(63) Van Beek, L. K. H. In *Progress in Dielectrics*; Birks, J. B., Ed.; Heywood: London, 1967; p 69.
(64) Debye, P.; Pauling, L. *J. Am. Chem. Soc.* **1925**, *47*, 2129.
(65) Lai, J. R.; Fisk, J. D.; Weisblum, B.; Gellman, S. H. *J. Am. Chem. Soc.* **2004**, *126*, 10514.
(66) Paci, E.; Vendruscolo, M. *J. Phys.: Condensed Matter* **2005**, *17*, S1617.
(67) Tekin, N.; Kadinci, E.; Demirbas, O.; Alkan, M.; Kara, A. *J. Colloid Interface Sci.* **2006**, *296*, 472.
(68) Latour, R. A., Jr.; Trembley, S. D.; Tian, Y.; Lickfield, G. C.; Wheeler, A. P. *J. Biomed. Mater. Res.* **2000**, *49*, 58.
(69) Gomez, C. M.; Codoner, A.; Campos, A.; Abad, C. *Int. J. Biol. Macromol.* **2000**, *27*, 291.
(70) Finette, G. M. S.; Mao, Q-M.; Hearn, M. T. W. *J. Chromatogr. A* **1997**, *763*, 71.
(71) Watanabe, H.; Ikoma, T.; Chen, G.; Monkawa, A.; Tanaka, J. *Key Eng. Mater.* **2006**, *309*−*311*., 533.
(72) Qi, Z.; Matsuda, N.; Takatsu, A.; Kato, K. *J. Phys. Chem. B* **2003**, *107*, 6873.
(73) Thuduppathy, G. R.; Craig, J. W.; Kholodenko, V.; Schon, A.; Hill, R. B. *J. Mol. Biol.* **2006**, 359, *1045.*
(74) Weisswange, I.; Bretschneider, T.; Anderson, K. I. *J. Cell Sci.* **2005**, *118*, 4375.
(75) Andersen, O. S.; Felberg, S.; Nakadomari, H.; Levy, S.; McLaughlin, S. *Biophys. J.* **1978**, *21*, 35.
(76) Ishiguro, R.; Yokoyama, Y.; Maeda, H.; Shimamura, A.; Kameyama, K.; Hiramatsu, K. *J. Colloid Interface Sci.* **2004**, *290*, 91.
(77) Keller, S.; Heerklotz, H.; Blume, A. *J. Am. Chem. Soc.* **2006**, *128*, 1279.
(78) Milanesi, L.; Petrillo, M.; Sepe, L.; Boccia, A.; D'Agostino, N.; Passamano, M.; Di Nardo, S.; Tasco, G.; Casaio, R.; Paolella, G. *BMC Bioinformatics* **2005**, *6*, supp. 4.
(79) Ori, H.; Nakamura, K. *Eur. J. Nucl. Med.* **1980**, *5*, 155.
(80) Baenziger, J. E.; Jarrell, H. C.; Smith, J. C. P. *Biochemistry* **1992**, *31*, 3377.
(81) Lyon, C. E.; Suh, E-S.; Dobson, C. M.; Hore, P. J. *J. Am. Chem. Soc.* **2002**, *124*, 13018.
(82) Silverman, B. D. *Proteins: Struct., Funct., Genet.* **2003**, *53*, 880.
(83) Zuckermann, M. J.; Heimburg, T. *Biophys. J.* **2001**, *81*, 2458.
(84) Heimburg, T.; Marsh, D. *Biophys. J.* **1995**, *68*, 536.
(85) Leggio, C.; Galantini, L.; Zaccarelli, E.; Pavel, N. V. *J. Phys. Chem. B* **2005**, *109*, 23857.
(86) Fleck, C.; Netz, R. R.; Von Gruber, H. H. *Biophys. J.* **2002**, *82*, 76.
(87) Hathcock, J. J.; Rusinovaa, E.; Gentry, R. D.; Andree, H.; Nemerson, Y. *Biochemistry* **2005**, *44*, 8187.
(88) Velev, O. D. *Adv. Biophys.* **1997**, *34*, 139.
(89) Pellenc, D.; Gallet, O.; Berry, H. *Phys. Rev. E* **2005**, *72*, 051904/1.
(90) Jalbert, L. R.; Chan, J.; Christiansen, W. T.; Castellino, F. J. *Biochemistry* **1996**, *35*, 7093.
(91) Watson, R. M.; Woody, R. W.; Lewis, R. V.; Bohle, D. S.; Andreotti, A. H.; Ray, B.; Miller, K. W. *Biochemistry* **2001**, *40*, 14037.
(92) Ciurleo, A.; Cinelli, S.; Guidi, M.; Bonincontro, A.; Onori, G.; La Mesa, C. *Biomacromolecules*, in press.
(93) Lu, R.-C.; Cao, A.-N.; Lai, L.-H.; Xiao, J.-X. *J. Colloid Interface Sci.* **2006**, *293*, 61.
(94) Moroi, Y. *Micelles: Theoretical and Applied Aspects*; Plenum Press: New York, 1992; Chapter X, p 183.
(95) Muzzalupo, R.; Gente, G.; La Mesa, C.; Caponetti, E.; Chillura-Martino, D.; Pedone, L.; Saladino, M. L. *Langmuir* **2006**, *22*, 6001.
(96) Krueger, C.; Jonas, U. *J. Colloid Interface Sci.* **2002**, *252*, 331.
(97) Jung, H. T.; Coldren, B.; Zasadzinski, J. A.; Iampietro, D. J.; Kaler, E. W. *Proc. Natl. Acad. Sci. U.S.A.* **2001**, *98*, 1353.